Preventive Energy Management Strategy Before Extreme Weather Events by Modeling EVs' Opt-In Preferences

Mohammad Reza Salehizadeh, *Senior Member, IEEE*, Ayşe Kübra Erenoğlu, *Member, IEEE*, İbrahim Şengör, *Senior Member, IEEE*, Akın Taşçıkaraoğlu, *Senior Member, IEEE*, Ozan Erdinç, *Senior Member, IEEE*, Jay Liu, and João P. S. Catalão, *Fellow, IEEE*

***Abstract*— In recent literature, the value of electric vehicles (EVs) for the resilience enhancement of urban microgrids has been shown. Furthermore, on a larger scale, there has been a growing recognition of the potential of EV cooperation in enhancing the overall resilience of smart cities. To this end, the city can be partitioned into a set of blocks, each encompassing buildings. Within each block, EV traveling time can be ignored. As a step forward, this study presents a Preventive Energy Management (PEM) strategy along with a rescheduling procedure by cooperation of EVs, local distributed energy resources (DERs), and buildings in different city blocks. Based on the available information related to the amount of curtailed loads, two cases are modeled and studied. In the proposed PEM strategy, EV owners' opt-in preferences such as arrival and departure times, and the city block in which they are willing to give energy services are modeled. As a more realistic consideration, the proposed model does not consider the buildings' load as a lumped load, instead the PEM strategy is designed to consider each of the buildings separately. The resulting optimization model is flexible enough to enable EVs to switch from one building to another to provide energy in different time slots. By applying disjunctive-constraint-based transformation, the model is recast as a Mixed Integer Linear Programming (MILP) that could be efficiently solved by commercial optimization solvers. The proposed approach is applied to a benchmark and the results are analyzed. According to the results, using EVs in the PEM strategy has been proven to be effective and the importance of the length of the period of service and opt-in preferences for optimal scheduling are highlighted.**

***Index Terms*— Distributed energy resources (DERs), electric vehicles, natural disasters, vehicle-to-building, vehicle-to-grid, urban resilience.**

Manuscript received 1 January 2024; revised 30 April 2024 and 14 June 2024; accepted 23 July 2024. The work of Mohammad Reza Salehizadeh and Jay Liu was supported by the National Research Foundation of Korea (NRF) Grant funded by the Korean Government [Ministry of Science and ICT (MSIT)] under Grant RS-2024-00337129. The work of Ozan Erdinç was supported by the 100th Year The Scientific and Technological Research Council of Turkey (TUBITAK) Science Encouragement Award. The Associate Editor for this article was C. K. Sundarabalan. *(Corresponding author: Jay Liu.)*

Mohammad Reza Salehizadeh is with the Institute of Cleaner Production Technology, Pukyong National University, Busan 48547, Republic of Korea (e-mail: salehizadeh@pknu.ac.kr).

Ayşe Kübra Erenoğlu and Ozan Erdinç are with Electrical Engineering Department, Yıldız Technical University, 34220 Istanbul, Türkiye (e-mail: erenayse@yildiz.edu.tr; oerdinc@yildiz.edu.tr).

İbrahim Şengör is with the Department of Electrical and Electronic Engineering, Munster Technological University, Cork, T12 P928 Ireland (e-mail: Ibrahim.Sengor@mtu.ie).

Akın Taşçıkaraoğlu is with the Department of Electrical and Electronics Engineering, Mugla Sitki Kocman University, 48000 Mugla, Türkiye, and also with the Electrical and Computer Engineering Department, University of California San Diego, San Diego, CA 92093 USA (e-mail: akintascikaraoglu@mu.edu.tr).

Jay Liu is with the Institute of Cleaner Production Technology, Pukyong National University, Busan 48547, Republic of Korea, and also with the Department of Chemical Engineering, Pukyong National University, Busan 48513, Republic of Korea (e-mail: jayliu@pknu.ac.kr).

João P. S. Catalão is with the Research Center for Systems and Technologies (SYSTEC), Advanced Production and Intelligent Systems Associate Laboratory (ARISE), Faculty of Engineering, University of Porto, 4200-465 Porto, Portugal (e-mail: catalao@fe.up.pt).

Digital Object Identifier 10.1109/TITS.2024.3435049

Nomenclature

Abbreviations

DER	Distributed Energy Resource.
PEM	Preventive Energy Management.
EV	Electrical Vehicle.
ECSC	Energy Coordinator of Smart City.
TSO	Transmission System Operator.
DSO	Distribution System Operator.
SoE	State-of-Energy.
V2G	Vehicle-to-Grid.
MILP	Mixed Integer Linear Programming.

Indices

e	Index of EV.
b	Index of building.
t	Index of time.
bl	Index of block.

Sets

T	Set of times in extreme weather event period.
B	Set of buildings.
E	Set of EVs.
B_{bl}	Set of buildings in block bl.
E_{bl}	Set of EVs giving services in block bl.
T_{RESCH}	Set of rescheduling periods.
B_{RES}	Set of affected buildings by power mismatch due to uncertainty.
S_b	Set of parties who simultaneously cause a mismatch in building b.

Parameters

$P^{CUR}_{TOTAL,t}$	Total load curtailment at time t in Case A [kW].
DiR_e	Discharge rate of EV e [kW].
SoE^{ini}_e	Initial SoE of EV e [kWh].
SoE^{max}_e/SoE^{min}_e	Max/Min value of SoE of EV e [kWh].
$P^{DERmax}_{b,t}$	The upper bound of purchase power from local DER in building b at time t [kW].
$P^{CUR}_{b,t}$	The amount of load curtailment in building b at time t in Case B [kW].
ρ^{dis}_t	Discharge price at time t [$/kWh].
$\rho^{down}_{b,t}$	Price of decreasing power in building b at time t [$/kWh].
$P^{DERmax}_{b,t}$	Maximum power provided from local DER in building b at time t [kW].
$P^{Pmax}_{b,t}$	The upper bound of priority load curtailment in building b at time t [kW].
$P^{Dmax}_{b,t}$	The upper bound of discretionary load curtailment in building b at time t [kW].
DE_e	Discharge efficiency of EV e [%].
t^A_e	Arrival time of EV e.
t^D_e	Departure time of EV e.
$P^{CURmax}_{b,t}$	Maximum allowed value of the amount of load curtailment in building b at time t [kW].

Variables

$P^{dis}_{e,t}$	Discharge power of EV e at time t [kW].
$SoE_{e,t}$	State of energy of EV e at time t [kWh].
$P^{DER}_{b,t}$	Purchased power from local DER in building b at time t [kW].
$P^{D}_{b,t}$	The amount of load curtailment in building b at time t (in Case B) [kW].
$P^{D}_{TOTAL,t}$	The total amount of discretionary load decreasing in building b at time t (in Case A) [kW].
$P^{Pdown}_{b,t}$	The amount of priority load decreasing in building b at time t [kW].
$P^{Ddown}_{b,t}$	The amount of discretionary load decreasing in building b at time t [kW].
$\propto_{e,b,\mathrm{t}}$	A binary variable that is equal to one if the EV e is connected to building b at the time t.

I. Introduction

A. Motivation and Background

The number of individuals living in urban areas is expected to increase by 13% from 2018 to 2050 [1]. Recently, more than 200,000 people left without power across the Bay Area in San Francisco, California by strong wind storms [2] because the high density urban areas were unprepared for the extreme weather conditions and demonstrating the need for urban resilience which is defined as the capacity of an urban system and all its interconnected social, ecological, and technological networks to maintain or swiftly regain desired functions when faced with disruption [3]. Urban resilience also refers to the ability to adjust to changes and efficiently transform systems that hinder present or potential adaptability in both time and space.

Enhancing urban areas' resilience includes maintaining access to electrical energy when the electrical system has been affected by high-impact, low-probability (HILP) events. Some of these HILP events are related to digitalization in which the data-related infrastructure of cities encounters cyber-attacks. The others can be weather-based basis such as storms and floods and the ever-increasing occurrence can be due to global warming. Resiliency-oriented actions in a preventive, corrective, and restorative manner are required to guarantee the security and safety of urban areas and their related infrastructures in the case of the occurrence of HILP events. Reliable energy procurement for a city during the period of occurrence of extreme natural disasters is a serious challenge because transmission lines and distribution feeders are susceptible to outage due to various reasons, including fallen trees damaging power lines, and lightning strikes.

The objective of this study is to provide a day-ahead energy management strategy along with a rescheduling program to utilize EVs for enhancing urban area resilience. This is achieved by considering the opt-in/out behavior and location preferences for EV services.

B. Literature Review

Urban areas need to maintain access to electrical energy in the presence of HILP events such as natural disasters. The presented study improves urban resilience through a preventative strategy. The remainder of this literature review discusses current preventative work and is divided into two categories: *energy network-based actions,* and *load-sustaining focused actions*.

In the *first* category, the preventive actions that are adopted in a pre-disturbance state can be *long-term* or *short-term* [4]. In [4] microgrid-based planning and operation for resiliency improvement have been reviewed and classified. The *long-term actions* include network reinforcement, optimal planning, and installing new control devices such as Flexible Alternating Current Transmission System (FACTS). In [5], the objective is to construct a tri-level defense-attack model that can identify the optimal strategy for strengthening a distribution system against malicious attacks, considering the resources available for defense and operational restoration measures. In [5], based on the conducted numerical analysis, the manner in which operational resilience impacts system hardening is investigated. In [6], a planning strategy focusing on resilience is suggested for an active distribution network to be prepared for potential malicious attacks. The proposed strategy prioritizes the coordination of line hardening and signal protection to minimize both direct and indirect failures. To introduce a framework for improving the resilience of a distribution network, a two-stage stochastic MILP model is presented in [7]. In the first stage, investments are made in multiple strategies such as strengthening power lines, implementing dispersed generators, allocating mobile emergency producers, and deploying switches. The objective of [8] is to present a trilevel optimization model aimed at enhancing the resilience of both transmission lines and communication cables through hardening. The study demonstrates that cyber-topology interdependence can lead to increased load losses and significantly impact the effectiveness of hardening strategies. In [9], an approach based on the scenario degree of severity index is presented to enhance resilience in power systems. The proposed approach allows power grid planners to efficiently manage multiple resilience metrics in a multi-objective decision-making model. The proposed method is demonstrated by applying it to determining the optimal allocation of the thyristor-controlled series compensator (TCSC).

The purpose of [10] is to present a multi-stage robust optimization approach that can effectively schedule regional power grids in the face of tropical cyclones. Taking into account the uncertainties over time, a resiliency-oriented scheduling model is developed to identify proactive strategies and response plans both before and following the occurrence of uncertainties. In [11], a two-step programming approach is proposed, which is based on a resilience-oriented model, for the design of micro-turbines, photovoltaic (PV) panels, and mobile batteries in a multi-energy microgrid. The aim is to enhance the system's ability to withstand high-intensity events. This framework is developed as a mixed integer quadratic program. It involves decision-making in investment in the first stage and optimizing operational variables in the second stage, all geared towards strengthening the system's resilience.

A few related works from *short-term actions* can be mentioned: In [12], an attempt is made to improve the resilience of distribution systems against earthquakes using a mobile battery storage system. Additionally, a seismic model is introduced, which considers not only the direct effects of earthquakes but also the influence of building damage around distribution networks on power poles. To increase the resilience of power networks during typhoons, [13] develops a three-stage resiliency-oriented unit commitment model that considers the stochastic nature of typhoon paths and line failures, while coordinating preventive control, emergency control, and restoration efforts. A two-stage emergency-focused dispatch model for maximizing power system operations in harsh circumstances is presented in [14]. The suggested model integrates renewable energy, thermal power generation, and energy storage into its approach through thorough case analysis utilizing real data. To enhance the resilience of transportation-power distribution systems during extreme events, [15] introduces a coordinated optimization methodology for deploying emergency response resources within the networks. This approach coordinates the reversal of traffic links in transportation networks, power line switching in distribution networks, and management of fast charging stations' charging piles. The coordinated power-transportation distribution systems mathematical model is formulated as a Mixed Integer Non-Linear Programming problem based on the dynamic transportation networks model and the multi-period distribution system model. It is then transformed into a more computationally effective MILP problem by using linearization methods.

Reference [16] presents a novel approach to robust scheduling of electricity-hydrogen distribution networks in the event of catastrophic events: a risk-constrained trilevel MILP formulation. An enhanced nested column-and-constraint generation technique is designed to compute the trilevel optimization program with discrete decisions in innermost level issues effectively.

In the *second* category, a set of preventive actions such as using local distributed energy resources (DERs) and EVs are adopted to sustain loads [17], [18]. Reference [17] introduces a distributed control strategy designed for a fleet of EVs, aimed at bolstering the resilience of an urban energy system in the face of extreme contingencies. Reference [18] explores the benefits of enhancing resilience through smart vehicle-to-grid (V2G) control, the significance of electric vehicle owner cooperation for system resilience, and the synergistic effects of photovoltaic (PV) and EV interaction within an urban multi-energy microgrid. To improve resiliency, in [19], the performance of a battery/PV system is simulated for healthcare centers situated in the Rohingya refugee camp in Bangladesh. Reference [20] presents a strategy for residential buildings to sustain self-powered operations during scheduled grid outages by utilizing plug-in hybrid electric vehicles (PHEVs) as backups for residential PV systems, integrating the load-shifting capabilities of smart homes, and employing a stochastic programming approach to manage uncertainty in residential PV solar power generation.

The attention to the role of EVs in resilience improvement has increased in recent years. EV discharging is used as both network-based actions [21], and load-sustaining focused actions [18], [22]. Also, they are used as preventive [22] or restorative actions [21]. A resiliency-oriented, multi-stage critical load restoration approach for distribution systems integrating on-call EVs under the fleet operator framework in advance of a high-intensity load replacement event is proposed in [21]. The primary focus of the model is to maximize the cumulative service time of demands weighted by load priority with the lowest possible number of EVs. In [22], coordination between EV battery and reserve battery has been performed for resilience improvement. As another endeavor outlined in [23], critical load restoration and energy loss minimization during natural disasters are achieved through a shared EV parking lot.

In the scale of a smart city, sustaining loads in urban areas via EV discharging is an effective way to improve resilience. By 2030, it is desired to have a 50% market share for EV sales in the U.S. [24]. As a feasible solution, based on the presented definition of urban resilience, a coordinated fleet of EVs with the cooperation of their owners can be considered as a "socio-technical network" that can help smart cities on the temporal and spatial scale to be returned to its desired energy function in the case of occurrence of a contingency. As mobile emergency resources, EVs could be scheduled to give energy services to different urban areas during extreme periods. The value of EV coordination for resilience improvement is assessed in [18] wherein two categories (individual-prioritized and system-prioritized) are defined based on their SoE preferences for EV participation in resiliency-oriented V2G. In the proposed PEM strategy, this point is considered more comprehensively because the EVs are asked to offer their minimum desirable SoE ($\mathrm{SoE}_{\mathrm{min}}$). $\mathrm{SoE}_{\mathrm{min}}$ would be applied to avoid range anxiety. In addition, arrival time, departure time, and the block of city that they are willing to give energy service are included in the modeled opt-in preferences that we consider in the PEM strategy.

Table I compares the features of this paper with EV-related papers aimed at enhancing resiliency. From the literature review above, the following research gaps are observed:

- None of the aforementioned studies precisely models EV preferences.
- None of the aforementioned studies models the opt-in/out aspect presented in this model.
- None of the resiliency-related studies considers different prediction scenarios for load curtailments at the building level or aggregative level of buildings in city blocks.

To address all of these gaps, this paper proposes a day-ahead energy management strategy along with a rescheduling program to utilize EVs for enhancing urban area resilience. This includes modeling the opt-in/out behavior and location of service preferences of EVs.

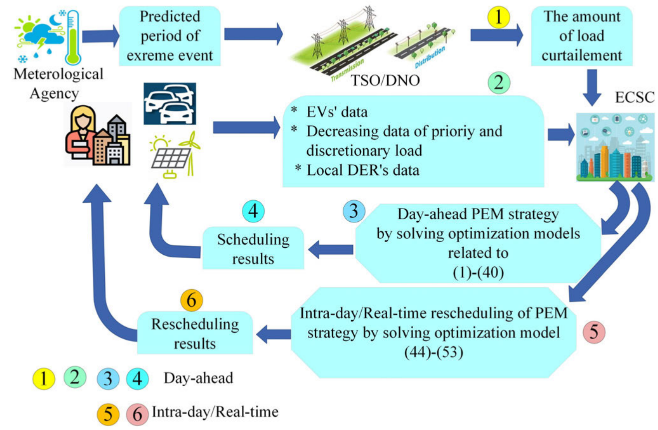

Fig. 1. The proposed PEM strategy.

C. Regulatory Consideration

Energy management in a smart city involves the coordination and aggregation of various components such as generation, distribution, consumption, and storage facilities. In this paper, we consider the Energy Coordinator of Smart City (ECSC) as an entity other than DSO. While the DSO plays a crucial role in managing the electricity distribution infrastructure, the ECSC is responsible for managing different aspects of energy in a smart city. This assumption is consistent with some real examples. The Borrego Springs microgrid in San Diego serves a community of customers wherein distribution network assets are managed by the utility, but the DERs are owned by customers and independent power producers [25].

Hu et al. [26] showed that extreme weather events are predictable at least 1 day ahead. In research performed in NREL [27], two machine-learning methods named ensemble boosted tree (EBT) and decision tree (DT) have been employed to predict outage possibility of recloser and substation. By having such information, through power flow analysis, it is possible to predict the amount of load curtailment in different nodes of the distribution network and city blocks. Also, in [28], a logistic regression model is used to forecast weather-related day-ahead outage power. According to this, in Step 1 of Fig. 1, we assume that the amount of load curtailment due to the extreme weather event is predictable.

MIT researchers demonstrated the value of V2G in transition to a low-carbon energy system in the case of the New England power system [29]. That research shows that by just 13.9% of participation in the V2G program, over $700 million in savings would be obtained. However, despite being technologically mature, owners' willingness to participate in V2G is not enough yet. A survey in Germany conducted by Geske and Schumann [30] shows that a non-monetary factor "range anxiety" i.e., fear of running out of SoE is the dominant reason for unwillingness to participate in the V2G program. In this paper, to tackle this obstacle, the EV owners are enabled to choose $\mathrm{SoE}_{\min}$ as an opt-in preference. On the other hand, the role of monetary incentives for V2G promotion is confirmed in Norway [31]. In this regard, we consider a price signal for rewarding EV owner's participation in the proposed PEM strategy. Apart from the aforementioned policy recommendations that we will include in our proposed REVF-SCH model, the participation of EVs in extreme conditions is not far from reality in recent years. The experience of the 2021 Texas winter storm shows that people may not be willing to participate in normal conditions for giving energy service, but they show a higher willingness to participate in extreme periods [32]. As another contribution of other mobile resources in resiliency enhancement, a mobile hydrogen energy resource "Hornet" preserved the essential loads for six hours during the strike of Super Typhoon in China [16].

Performing Steps 2,4 and 6 of the PEM strategy requires proper communication technologies that allow communication between ECSC and the between ECSC and the participants, especially EVs. There are a few ways such as using cellular networks, such as 4G or 5G, and IoT platforms and protocols, such as Message Queuing Telemetry Transport (MQTT) or Constrained Application Protocol (CoAP). Also, Advanced Metering Infrastructure (AMI) technologies like smart meters enable ECSC to gather real-time data on the electricity consumption of buildings.

D. Contributions and Highlights

The major contributions of this work are summarized as follows:

- For the first time, an optimal PEM strategy is designed for improving urban areas' resiliency against extreme weather events by coordination of EV fleet, buildings, and local DERs.
- The detailed EV preferences including opt-in and opt-out (arrival and departure time) are modeled in the proposed strategy.
- The optimal strategy is designed in a way to include this possibility for EVs to give energy service to all buildings located in an urban area in their service time.
- The proposed strategy is formulated for two cases: In Case A, the ECSC is asked to curtail the total amount of load in the city blocks under its management each time during an extreme weather event period. In contrast to

Case A, in Case B, the amount of load curtailment is given to ECSC for each of the buildings.

In other words, our work uncovers EV owners' opt-in preferences for increasing the value of Vehicle-to-Building (V2B) for resilience enhancement.

E. Organization

After presenting the Introduction in Section I, the developed PEM strategy is brought in Section II. Section III describes numerical analysis by presenting a set of associated tests that are used to discuss the results. Finally, the conclusion and a set of suggestions are given in Section IV.

II. PEM Strategy

A holistic view of the proposed scheme, along with the assumptions of the problem is presented in subsection A. The detailed mathematical model of the proposed PEM strategy for Case A is presented in Subsection B. Then, the linearization of the model using disjunctive-constraint-based transformation is brought in Subsection C. The modeling consideration for Case B is presented in Subsection D. As the day-ahead program might require modifications because of the possible uncertainties, the relevant mathematical model is provided in Subsection E.

A. The Proposed Scheme

It is assumed that the smart city is partitioned into a set of city blocks with a set of buildings and the traveling time of EVs inside each of them is ignorable. From an energy resilience perspective, finer spatial scale partitioning can be performed than what exists by integrating various energy-related criteria. However, it is out of the scope of this paper. In this study, we assume that through a set of incentive mechanisms, a set of EVs participate in PEM. The design of incentive mechanisms requires a set of socio-techno studies that is out of the scope of our study. It is also assumed that the amount of load curtailment for Cases A and B is given to the ECSC. Figure 1 shows the overall scheme of the proposed approach. It is mentioned that in most countries, the responsibility for predicting extreme weather events falls under the authority of national meteorological agencies or departments such as the National Oceanic and Atmospheric Administration (NOAA) in the U.S. Assume that it is predicted that a powerful extreme weather event such as a storm to occur between t_{ES} and t_{EE} in the next day. Based on the received information and power flow analysis, the TSO or DSO predicts the amount of load curtailment for buildings located in various urban areas. There are two cases: In Case A, the total amount of curtailed load for all buildings is given to ECSC and the ECSC should manage the shortage of power by using EVs' discharging, decreasing power of loads, and local DER's power. In Case B, the amount of load curtailment for each of the buildings is given to ECSC. The mathematical models for both of these cases are brought in the next subsections.

It is noted that a building may consist of different loads with different importance degrees. A Value of Resilience standard (VOR123) proposed by the Clean Coalition, considers three tiers for loads in resilience studies: i) Mission-critical, life-sustaining loads, ii) Priority loads, and iii) Discretionary loads [37], [38]. Based on this categorization, in this model, we do not consider mission-critical, life-sustaining loads for curtailment purposes.

It is preferred to curtail discretionary loads instead of priority loads such as lighting, electrical facilities for maintaining perishable food items, etc. After receiving the predicted amount of load curtailment data from TSO/DSO, the ECSC schedules to procure energy for buildings with the cooperation of EV owners, residents of the buildings inside the city blocks, and local DERs (Step 2 of Fig. 1). The residents could participate in non-essential load curtailments to procure energy for essential loads. The optimal decision of the ECSC is dependent on the cooperation of each party. Due to the following reasons, in this schedule, the challenge of ECSC is mostly related to the coordination of EVs: First, a high number of EV owners is required to participate. Second, as described in the next subsection, both monetary and non-monetary factors can hinder EV participation which is attempted to relieve in this paper.

The opt-in preferences, including all these important factors are integrated into the mathematical model (1)-(19) that is solved by ECSC (Step 3 of Fig. 1). By solving this optimization model, the day-ahead schedule for preventing energy outages in the city blocks is obtained, i.e., the amount of non-essential load curtailment in each city block, the building sequences in which each EV should give energy services, the amount of discharge/charge power in each time, the amount of power that should be delivered by each DER, and the amount of power to be purchased from the grid. The output variables are fed back to the participants (Step 4 of Fig. 1). Due to the uncertainties that may occur, a rescheduling plan (24)-(38) is designed and performed (Step 5 of Fig. 1) before the time of occurrence of the extreme weather event and the pertaining variables will be sent to the participants (Step 6 of Fig. 1).

B. Mathematical Model: Case A

$$\text{Min } C_{PEM}^{DA} = C_{EV}^{DA} + C_{DEC}^{DA} + C_{DER}^{DA} \tag{1}$$

$$s.t. \quad P_{b,t}^{RLC} - P_{b,t}^{IN} = 0 \; \forall b \in B, t \in T \tag{2}$$

$$0 \le P_{b,t}^{Pdown} \le P_{b,t}^{Pdown,max} \; \forall b \in B, t \in T \tag{3}$$

$$0 \le P_{b,t}^{Ddown} \le P_{b,t}^{Ddown,max} \; \forall b \in B, t \in T \tag{4}$$

$$0 \le P_{e,t}^{dis} \le DiR_e . opt_{e,t} \; \forall e \in E, t \in \left[t_e^A t_e^D \right] \tag{5}$$

$$\sum\nolimits_{b \in B} \propto_{e,b,t} \le 1 \; \forall e \in \text{E}, \text{t} \in \text{T} \tag{6}$$

$$SoE_{e,t} = SoE_e^{ini} \; \forall e \in E, t = t_e^A \tag{7}$$

$$SoE_{e,t} = SoE_{e,t-1} + \Delta SoE_{e,t}$$
$$\forall e \in E, t \in \left(t_e^A t_e^D \right], t > (t_e^A + 1) \tag{8}$$

$$SoE_e^{min} \le SoE_{e,t} \le SoE_e^{max} \; \forall e \in \text{E}, t \tag{9}$$

$$0 \le P_{b,t}^{DER} \le P_{b,t}^{DERmax} \; \forall b \in B, \text{t} \in \text{T} \tag{10}$$

$$\sum\nolimits_{b \in B} P_{b,t}^{CUR} = P_{TOTAL,t}^{CUR} \; \forall t \in T \tag{11}$$

$$0 \le P_{b,t}^{CUR} \le P_{b,t}^{CURmax} \; \forall b \in B, \text{t} \in \text{T} \tag{12}$$

TABLE I
TAXONOMY TABLE OF EV-BASED RESILIENCE IMPROVEMENT PAPERS

Ref.	Preventive/ restorative	System	Action Type	Term	Rescheduling consideration	EVs' Preferences		Range anxiety consideration	Different load curtailment prediction scenarios
						Opt-in/out consideration	Location of Service		
[16]	Preventive	Electricity-Hydrogen Distribution Network	Energy network-based actions	Short-term	No	No	No	No	No
[17]	Preventive	Multi-energy Microgrid	load-sustaining focused actions	Short-term	Yes	No	No	No	No
[18]	Preventive	Multi-energy Microgrid	load-sustaining focused actions	Short-term	No	No	No	No	No
[21]	Restorative	Distribution Network	Energy network-based actions	Short-term	No	No	No	No	No
[22]	Preventive	Building	load-sustaining focused actions	Short-term	No	No	No	No	No
[33]	Restorative	Distribution and Transportation Network	Energy network-based actions	Short-term	No	No	No	No	No
[34]	Restorative	Distribution Network	Energy network-based actions	Short-term	No	No	No	No	No
[35]	Preventive	Distribution and Transportation Network	Energy network-based actions	Short-term	No	No	No	No	No
[36]	Preventive	Building	load-sustaining focused actions	Short-term	No	No	No	No	No
This paper	Preventive	Urban areas	load-sustaining focused actions	Short-term	Yes	Yes	Yes	Yes	Yes

where

$$C_{EV}^{DA} = \sum\nolimits_{e \in E} \sum\nolimits_{t \in T} P_{e,t}^{dis} . \rho_t^{dis} \tag{13}$$

$$C_{DEC}^{DA} = \sum\nolimits_{b \in B} \sum\nolimits_{t \in \mathrm{T}} \times (P_{b,t}^{Pdown} . \rho_{b,t}^{Pdown} + P_{b,t}^{Ddown} . \rho_{b,t}^{Ddown}) \tag{14}$$

$$C_{DER}^{DA} = \sum\nolimits_{b \in B} \sum\nolimits_{t \in T} P_{b,t}^{DER} . \rho_{b,t}^{DER} \tag{15}$$

$$P_{b,t}^{RLC} = P_{b,t}^{CUR} - P_{b,t}^{Pdown} - P_{b,t}^{Ddown} \;\; \forall b \in B, t \in T \tag{16}$$

$$P_{b,t}^{IN} = P_{b,t}^{DER} + \sum\nolimits_{e \in E} \propto_{e,b,\mathrm{t}} DE_e . P_{e,t}^{dis} \;\; \forall b, t \in T \tag{17}$$

$$\Delta SoE_{e,t} = -\Delta T . \frac{P_{e,t}^{dis}}{DE_e} \;\; \forall e \in E, t \in \left(t_e^A t_e^D \right], t > (t_e^A + 1) \tag{18}$$

$$\propto_{e,b,\mathrm{t}} \leq M . opt_{e,t} . u_{e,b} . P_{e,t}^{dis} \;\; \forall e \in E, b \in B, \mathrm{t} \in \mathrm{T} \tag{19}$$

As indicated in (1), in this model, the cost function (C_{PEM}^{DA}) is composed of discharging cost of EVs (C_{EV}^{DA}), cost of decreasing power (C_{DEC}^{DA}), and the cost of purchased power from local DERs (C_{DER}^{DA}) which are denoted in (13)-(15), respectively. Each term has been assigned appropriate price-based weights in its respective equation. It is noted that the price assigned to priority loads in (14) should be much higher than that of discretionary loads ($\rho_{b,t}^{Pdown} \gg \rho_{b,t}^{Ddown}$). The power balancing for each building is guaranteed by (2) wherein residual load curtailment from each of the buildings ($P_{b,t}^{RLC}$) should be compensated by the inflow of power to that building ($P_{b,t}^{IN}$), i.e., for building b at time t, load curtailment minus priority and discretionary loads' decreasing should be equal to local DER's power plus total discharge power injection. The residual load curtailment (the amount of load curtailment minus the amount of priority and discretionary load decreasing) and the inflow power of each of the buildings are formulated in (16), and (17), respectively. In (17), the term of $\sum_e \propto_{e,b,\mathrm{t}} DE_e . P_{e,b,t}^{dis}$, which is the discharge power from the EVs to building b at time t, is non-linear because of having the product of variables $P_{e,b,t}^{dis}$ and $\propto_{e,b,\mathrm{t}}$. In the next subsection, we recast (17) by a set of linear expressions. It is noted that $\propto_{e,b,t}$ will be zero if the EV e is not willing to give service at time t ($opt_{e,t} = 0$) and/or building b ($u_{e,b} = 0$). Also, $\propto_{e,b,t}$ will be zero if there is no discharge at time t. To guarantee these points, (19) is considered in the model, where M is a big number. The amount of decreased priority and discretionary loads of each building should be less than or equal to an upper limit prescribed by the building managers as in (3) and (4), respectively. Equation (5) implies that the discharging power of each EV should be less than or equal to the discharge rate of each EV, respectively. As previously stated, we define a binary parameter $opt_{e,t}$ which is equal to 1 if the EV e declares readiness to participate in energy service at time t. Thus, if $opt_{e,t}$ is zero, $P_{e,t}^{dis}$ becomes zero, i.e., the EV e would not provide energy service at time t.

To ensure that each EV at a specific hour could be connected to a maximum of one building, inequality of (6) is included in the proposed mathematical model. Equations (7)-(9) describe the SoE of EV. The initial value of SoE of each EV is assigned by (7). SoE of EV changes in an interval when the EV battery is discharged. As represented in (8), the SoE of EV at time t is equal to the SoE at *t-1* plus the change of SoE due to discharging in that interval ($\Delta SoE_{e,t}$). The expression of $\Delta SoE_{e,t}$ is denoted in (18) wherein ΔT is time granularity and must be in second. The SoE of each EV battery lies within a predetermined limit, as modeled in (9). SoE_e^{min} can be set by considering the EV's desired SoE at the departure time. The injected power from local DERs to the buildings ($P_{b,t}^{DER}$) might be limited at each time. Equation (10) adds this constraint to the optimization model. In Case A, the total amount of load curtailment for all city blocks at each time ($P_{TOTAL,t}^{CUR}$) is given to the ECSC. The assigned curtailment to each building at time t ($P_{b,t}^{CUR}$) should be obtained in a way that (11) is satisfied. Moreover, an upper bound for $P_{b,t}^{CUR}$ should be considered in (12) where the upper bound of $P_{b,t}^{CUR}$ ($P_{b,t}^{CURmax}$), is less than $\sum_b (P_{b,t}^{Pmax} + P_{b,t}^{Dmax})$. It is mentioned that even if the amount of energy reserve provided by EVs is not sufficient, the model is still capable of managing resilience by decreasing power or by DER penetration.

C. Equivalent Linear Problem

Because of the nonlinear equation of (17), the mathematical model is not MILP. To substitute (17) with a few equivalent linear expressions, by getting inspiration from previous studies ([39], [40]), we apply disjunctive-constraint-based transformation and substitute $\propto_{e,b,t} DE_e.P_{e,t}^{dis}$ by a positive variable $P_{e,b,t}^{INJ}$ in (17):

$$P_{e,b,t}^{INJ} = \propto_{e,b,t} DE_e.P_{e,t}^{dis} \ \forall \text{e, b,} t \tag{20}$$

Also, the following linear expressions are added to the model:

$$P_{e,b,t}^{INJ} - DE_e.P_{e,t}^{dis} \leq N.(1 - \propto_{e,b,t}) \ \forall \text{e, b,} t \tag{21}$$

$$-\text{N}.(1 - \propto_{e,b,t}) \leq P_{e,b,t}^{INJ} - DE_e.P_{e,t}^{dis} \ \forall \text{e, b,} t \tag{22}$$

$$0 \leq P_{e,b,t}^{INJ} \leq DE_e.DiR_e.\propto_{e,b,t} \ \forall \text{e, b,} t \tag{23}$$

If the EV e gives energy to building b at time t, $\propto_{e,b,t}$ would be equal to 1. Then, the RHS of (21) and the LHS of (22) become zero. Hence, $P_{e,b,t}^{INJ} - DE_e.P_{e,t}^{dis} = 0$. Also, $P_{e,b,t}^{INJ}$ would be zero for $\propto_{e,b,t} = 0$. By considering (23), if $\propto_{e,b,t} = 0$, we have $P_{e,b,t}^{INJ} = 0$. If $\propto_{e,b,t} \neq 0$, the lower and upper bounds of $P_{e,b,t}^{INJ}$ would be equal to those of $DE_e.P_{e,t}^{dis}$.

D. Modeling Considerations in Case B

In comparison to Case A, Case B provides the ECSC with a higher level of detailed information. In Case B, the amount of load curtailment for each building at each time ($P_{b,t}^{CUR}$) is given as input data. Hereby, (11) and (12) are omitted from the model. From a mathematical modeling perspective, the feasible set of the optimization model will be a few sets whose intersections are empty. To show that let us redefine the sets of resultant optimization model ((1)-(10), (13)-(19)): BL is the set of city blocks, B_{bl} is the set of buildings in city block bl. E_{bl} is the set of EVs that give energy service to block bl. For more clarification, we re-write the model for Case B ((1)-(10), (13)-(19)) with the newly defined sets:

$$\text{Min} \quad C_{PEM}^{DA} = C_{EV}^{DA} + C_{DEC}^{DA} + C_{DER}^{DA} \tag{24}$$

$$s.t. \quad P_{b,t}^{RLC} - P_{b,t}^{IN} = 0 \ \forall t \in T, b \in B_{bl}, \text{bl} \in \text{BL} \tag{25}$$

$$0 \leq P_{b,t}^{Pdown} \leq P_{b,t}^{Pdown,max} \quad \forall t \in T, b \in B_{bl}, \text{bl} \in \text{BL} \tag{26}$$

$$0 \leq P_{b,t}^{Ddown} \leq P_{b,t}^{Ddown,max} \quad \forall t \in T, b \in B_{bl}, \text{bl} \in \text{BL} \tag{27}$$

$$0 \leq P_{e,t}^{dis} \leq DiR_e.opt_{e,t} \quad \forall t \in \left[t_e^A t_e^D\right], e \in E_{bl}, \text{bl} \in \text{BL} \tag{28}$$

$$\sum\nolimits_{b \in B_{bl}} \propto_{e,b,t} \leq 1 \ \forall \text{t} \in \text{T}, e \in E_{bl}, \text{bl} \in \text{BL} \tag{29}$$

$$SoE_{e,t} = SoE_e^{ini} t = t_e^A, \ \forall e \in E_{bl}, \text{bl} \in \text{BL} \tag{30}$$

$$SoE_{e,t} = SoE_{e,t-1} + \Delta SoE_{e,t} \quad \forall t \in \left(t_e^A t_e^D\right], t > (t_e^A + 1), e \in E_{bl}, \text{bl} \in \text{BL} \tag{31}$$

$$SoE_e^{min} \leq SoE_{e,t} \leq SoE_e^{max} \quad \forall t \in \left[t_e^A t_e^D\right], e \in E_{bl}, \text{bl} \in \text{BL} \tag{32}$$

$$0 \leq P_{b,t}^{DER} \leq P_{b,t}^{DERmax} \quad \forall t \in T, b \in B_{bl}, \text{bl} \in \text{BL} \tag{33}$$

where

$$C_{EV}^{DA} = \sum\nolimits_{\text{bl} \in \text{BL}} \sum\nolimits_{e \in E_{bl}} \sum\nolimits_{t \in \text{T}} P_{e,t}^{dis}.\rho_t^{dis} \tag{34}$$

$$C_{DEC}^{DA} = \sum\nolimits_{bl \in BL} \sum\nolimits_{b \in B_{bl}} \sum\nolimits_{t \in \text{T}} \times (P_{b,t}^{Pdown}.\rho_{b,t}^{Pdown} + P_{b,t}^{Ddown}.\rho_{b,t}^{Ddown}) \tag{35}$$

$$C_{DER}^{DA} = \sum\nolimits_{bl \in BL} \sum\nolimits_{b \in B_{bl}} \sum\nolimits_{t \in \text{T}} P_{b,t}^{DER}.\rho_{b,t}^{DER} \tag{36}$$

$$P_{b,t}^{RLC} = P_{b,t}^{CUR} - P_{b,t}^{Pdown} - P_{b,t}^{Ddown} \quad \forall t \in T, b \in B_{bl}, \text{bl} \in \text{BL} \tag{37}$$

$$P_{b,t}^{IN} = P_{b,t}^{DER} + \sum\nolimits_{bl \in BL} \sum\nolimits_{e \in E_{bl}} \propto_{e,b,t} DE_e.P_{e,t}^{dis} \quad \forall t \in T, b \in B_{bl}, \text{bl} \in \text{BL} \tag{38}$$

$$\Delta SoE_{e,t} = -\Delta T.\frac{P_{e,t}^{dis}}{DE_e} \ \forall t \in \left(t_e^A t_e^D\right], \quad t > (t_e^A + 1), e \in E_{bl}, \text{bl} \in \text{BL} \tag{39}$$

$$\propto_{e,b,t} \leq \text{M}.opt_{e,t}.u_{e,b}.P_{e,t}^{dis} \quad \forall t \in \text{T}, e \in E_{bl}, b \in B_{bl}, \text{bl} \in \text{BL} \tag{40}$$

In Case B, equations (24)-(33) correspond to equations (1)-(10) in Case A, respectively. Similarly, equations (34)-(40) correspond to equations (13)-(19), respectively. To streamline the presentation, detailed descriptions are referenced in the previous subsection for brevity. In all constraints ((25)-(40)), we index bl which belongs to set BL ($bl \in$ BL). Hence, the feasible set is separable for all blocks. On the other hand, from (34)-(36), it is understood that the objective (cost) function (24) is the sum of cost functions belonging to each city block. In this way, we have the following compact representation of the model for Case B:

$$\text{Min} \quad C_{PEM}^{DA} = \sum\nolimits_{bl \in BL} C_{PEM}^{DA}(X_{bl}) \tag{41}$$

$$s.t. \quad F(X_{bl}) = 0 \ \forall \text{bl} \in \text{BL} \tag{42}$$

$$G(X_{bl}) \leq 0 \ \forall \text{bl} \in \text{BL} \tag{43}$$

where (41) is the compact form of objective function (24), (42) is the compact form of (25), (30), (31), (37), and (38). Also, (43) is the compact form of (26)-(29), (32), (33), and (40). X_{bl} is a vector that represents the corresponding variables of Case B in Block bl. The optimization (41)-(43) can be separately solved for each block (bl $\in$ BL) and the related variables are obtained. Since the optimization models for all blocks are solved in parallel and the size of the problem is reduced, the solution speed will be decreased substantially in comparison to Case A.

E. Rescheduling

At any time from day-ahead to real-time, if the ECSC is notified that the parameters of the model deviate from what is inserted in the primary DA scheduling model, rescheduling should be performed. The deviated parameters can be about one or more than one party such as EVs, buildings, and local DERs.

Assume that the ECSC is informed that EVe will arrive with delay and its arrival time will be t_e^{A2} instead of t_e^{A1}, where $t_e^{A1} \leq t_e^{A2}$. Hence, in $\left[t_e^{A1} t_e^{A2}\right]$, rescheduling should be performed. If ECSC is notified that a delay in the arrival time will occur for more than one EV that is in the same city block, rescheduling needs to be performed in the affected periods. Assume $T_{e1}^{sch} = \left[t_{e1}^{A1} t_{e1}^{D1}\right]$ and $T_{e2}^{sch} = \left[t_{e2}^{A1} t_{e2}^{D1}\right]$ are the scheduled periods of EV1 and EV2 energy service. EV1 and EV2 arrive with delay i.e., t_{e1}^{A2} and t_{e2}^{A2}. The affected periods that require rescheduling are $\left[t_{e1}^{A1} t_{e1}^{A2}\right]$ and $\left[t_{e2}^{A1} t_{e2}^{A2}\right]$. If there is an intersection between these periods, cost allocation among the parties should be performed.

Since the rescheduling should be performed with fewer changes in the day-ahead PEM strategy, it is performed just in the corresponding buildings where that power balance has been deviated. In the rescheduling procedure, neither the EV traveling path nor the amount of discharge power in each period should change because changes in the discharge power of an EV at time t affect its SoE in the next periods [t t_e^D] and consequently the schedule of the next periods. To maintain the schedule with minimum change, the EVs should not participate in the rescheduling program. In this regard, we have three types of decision variables: the decreasing power in each building's primary and discretionary loads, and power produced by local DERs. For time t which belongs to the rescheduling period ($t \in T_{RESCH} = \left[t_1^{RESCH} t_2^{RESCH}\right]$), the following model can be solved in each affected building $b \in B_{RES}$:

$$\text{Min} \quad C_{PEMb,t}^{RESCH} = C_{DECb,t}^{RESCH\_P} + C_{DECb,t}^{RESCH\_D} + C_{DERb,t}^{RESCH} \tag{44}$$

$$s.t. \quad P_{b,t}^{OF-IN} - P_{b,t}^{RESCH} = 0 \tag{45}$$

$$0 \leq P_{b,t}^{RESCH\_Pdown} \leq P_{b,t}^{Pdown,max} - P_{b,t}^{Pdown} \tag{46}$$

$$0 \leq P_{b,t}^{RESCH\_Ddown} \leq P_{b,t}^{Ddown,max} - P_{b,t}^{Ddown} \tag{47}$$

$$0 \leq P_{b,t}^{RESCH\_DER} \leq P_{b,t}^{DERmax} - P_{b,t}^{DER} \tag{48}$$

where

$$C_{DECb,t}^{RESCH\_P} = P_{b,t}^{RESCH\_Pdown} . \rho_{b,t}^{RESCH\_Pdown} \tag{49}$$

$$C_{DECb,t}^{RESCH\_D} = P_{b,t}^{RESCH\_Ddown} . \rho_{b,t}^{RESCH\_Ddown} \tag{50}$$

$$C_{DERb,t}^{RESCH} = P_{b,t}^{RESCH\_DER} . \rho_{b,t}^{RESCH\_DER} \tag{51}$$

$$P_{b,t}^{RESCH} = P_{b,t}^{RESCH\_Pdown} + P_{b,t}^{RESCH\_Ddown} + P_{b,t}^{RESCH\_DER} \tag{52}$$

where

$$P_{b,t}^{OF-IN} = P_{b,t}^{OF} - P_{b,t}^{IN} \tag{53}$$

In the above model, the power imbalance ($P_{b,t}^{OF-IN}$), $P_{b,t}^{down}$, $P_{b,t}^{DER}$, $P_{b,t}^{Pdown}$, and $P_{b,t}^{Ddown}$ are given from solving the day-ahead PEM optimization of II-B or II-D. The rescheduling cost of (44) is minimized subject to constraints (45)-(3). Equation (45) ensures power balance in the affected building b. In this building, the imbalance of power ($P_{b,t}^{OF-IN}$) obtained from day-ahead scheduling (53) is compensated by rescheduling power. Equations (46)-(48) maintain the upper bound of the rescheduled power for priority load, discretionary load, and DER, respectively. Equations (49)-(51) show the terms of the objective function. According to (52), rescheduled power can be obtained from priority load, discretionary load, and DER, respectively. It is mentioned that similar to any rescheduling scheme in power systems, the prices used in the rescheduling phase are much higher than those used in the day-ahead scheduling i.e. $\rho_{b,t}^{DER} \ll \rho_{b,t}^{RESCH\_DER}$, $\rho_{b,t}^{Pdown} \ll \rho_{b,t}^{RESCH\_Pdown}$, and $\rho_{b,t}^{Ddown} \ll \rho_{b,t}^{RESCH\_Ddown}$.

The total rescheduling cost $\sum_{b \in B_{RES}} \sum_{t \in T_{RESCH}} C_{PEMb,t}^{RESCH}$ should be allocated among the parties that cause uncertainty. A simple procedure that can be adopted is to solve the rescheduling model (4)-(3) by considering only contingency about each party. Hereby, the rescheduling cost will be $C_{i,b,t}$ $\forall i \in S_b$, where S_b in the set of parties who simultaneously cause a mismatch in building b. A straightforward way to allocate the cost among them is to calculate the share of each of them as $\sum_{b \in B_{RES}} \sum_{t \in T_{RESCH}} \frac{C_{i,b,t}}{\sum_{i \in S_b} C_{i,b,t}} \bullet C_{PEMb,t}^{RESCH}$.

III. Numerical Analysis

The proposed PEM strategy is implemented to a benchmark with a few related tests. The devised mathematical models that are used in the PEM strategy are solved via GAMS v. 44.2.0 language with solver CPLEX v.22.1.1.0 [41]. Also, we use MATLAB v. R2023a, and Excel 365 for analysis and demonstrating data. All simulations are performed on a server with a 64-core 9.9 GHz CPU and 256.0 GB RAM. After presenting data in subsection A, the results and discussions are provided in subsection B. Scalability analysis and comparison tests are presented in subsections C and D, respectively.

A. Data and Assumptions

Assume that the ECSC is notified by the TSO/DSO that there will be an energy interruption in two city blocks due to a storm from 18:00 to 00:00 tomorrow. The schematic for the city blocks is shown in Fig. 2. Assume that each city block contains 4 buildings. In other words, 8 buildings are predicted to be affected by the storm. The ECSC invites the EV owner to participate in the PEM. Assume EV1-EV5 participate in city block1 and EV6-EV10 participate in city block2.

Figure 3 illustrates the opt-in preference of EVs for providing energy service in each interval. In this figure, the arrival and departure time of each EV (t_e^A and t_e^D) are depicted. As depicted in Fig. 3, the period of maximum EV participation

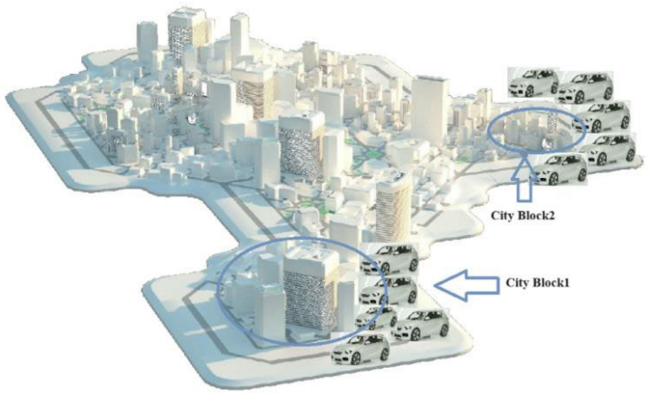

Fig. 2. EVs' locational willingness-to-participation.

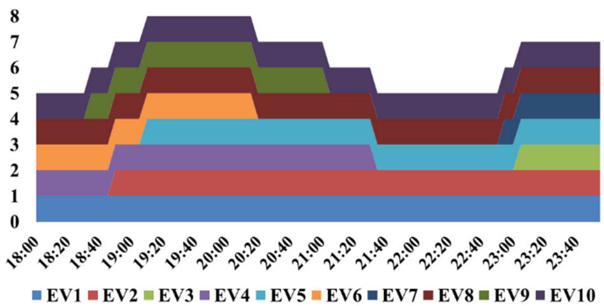

Fig. 3. Opt-in preference of EVs.

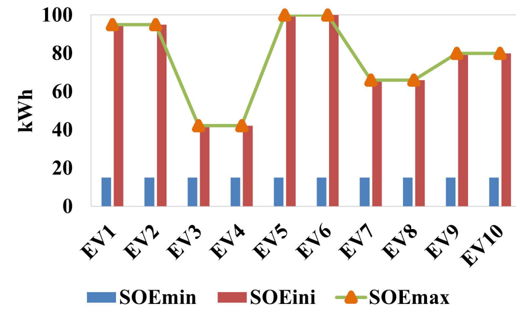

Fig. 4. $\mathrm{SoE_{min}}$, $\mathrm{SoE_{ini}}$, $\mathrm{SoE_{max}}$.

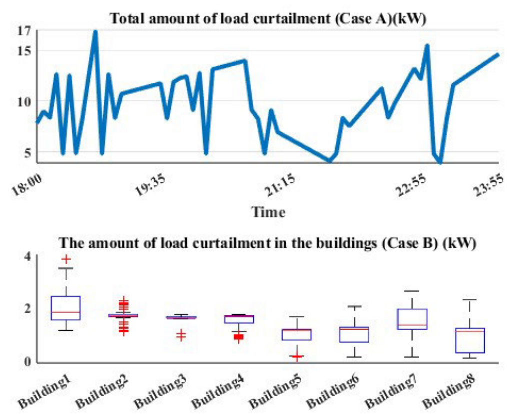

Fig. 5. Load curtailment for Cases A and B.

is from 19:10 to 20:15, during which 8 EVs are willing to participate in the PEM. Also, 50% of EVs' arrival time is 18:00. The average time that all EVs are willing to give energy service is 230.5 minutes. The average duration for blocks 1 and 2 are 246 and 215 minutes, respectively. Assume that the participating EVs have specifications of Audi e-Tron, BMW i3, Tesla Model X, Chevrolet Bolt, and Mercedes EQC. Hence, we have 10 EVs from each brand, as shown in Table II.

The maximum SoE and charging rate of each EV are given in Table III of [42]. Each EV determines its minimum SoE to mitigate range anxiety, which has been identified as a barrier to V2G participation [30]. The values of minimum, maximum, and initial SoE of each EV (SoE_e^{min}, SoE_e^{max}, and SoE_e^{ini}) indicated by each EV are shown in Fig. 4. We consider that $SoE_e^{min} = 15$ kWh for all EVs and the initial SoE is equal to the maximum SoE value which means EVs with their best initial SoE participate in the energy service program. The difference between SoE_e^{ini} and SoE_e^{min} can indicate the operational capacity ($OC_e = SoE_e^{ini} - SoE_e^{min}$ $\forall$e $\in$ E) of EV e in the PEM. In this regard, the Operational Capacity (OC) of EVs in block bl can be defined as $\sum_{e\in E_{bl}} OC_e / \sum_{e\in \mathrm{E}} OC_e$. Based on the assumptions made in this case study, EVs' OC would be equal to 48.5724% and 51.4276% for city blocks 1 and 2, respectively. It is observed that the OC of EVs is very close in two blocks.

For Case A, the total load curtailment ($P_{TOTAL,t}^{CUR}$) is shown in Fig. 5. As indicated, the maximum value is 16.848 kW which is related to the curtailment load of Building 1 at 18:45. It is assumed that the buildings in each city block are near enough to each other that the traveling time of EVs is negligible. In this numerical analysis, time granularity is considered 5 minutes. Hence, by considering the extreme period from 18:00 to 00:00, we have 72 times.

For Case B, the load curtailment for each building is depicted in Fig. 5. In each building, maximum priority and discretionary load curtailment would be $P_{b,t}^{Pdown,max}$ and $P_{b,t}^{Ddown,max}$, respectively. By demanding load curtailment from the TSO/DSO side, the building energy management would be under pressure. The more is $\frac{P_{b,t}^{CUR}}{P_{b,t}^{Pdown,max}+P_{b,t}^{Ddown,max}}$, the severity of curtailment would be higher from the perspective of energy management. Based on this, we can define a Curtailment Degree of Severity as:

$$CDS\,(b,t) = \frac{P_{b,t}^{CUR}}{P_{b,t}^{Pdown,max} + P_{b,t}^{Ddown,max}} \tag{54}$$

It is possible to consider weights for priority and discretionary upper bounds in the denominator. As mentioned previously, we did not allow priority load curtailment at this stage of the study. Since the number of buildings in each block is 4, the average of $\bar{CDS}(b,t)$ over time and the building of each city block is $\frac{\sum_b \sum_t CDS(b,t)}{72*4}$.

$CDS\,(b,t) = \frac{P_{b,t}^{CUR}}{P_{b,t}^{Pdown,max}+P_{b,t}^{Ddown,max}}$ The value of $\bar{CDS}(b,t)$ for city Blocks 1 and 2 is equal to 0.212446. In this way, it is assumed that the average curtailment degree of severity is considered equal for two city blocks.

TABLE II
EV BRANDS

Brands	EVs
Audi e-Tron	1,2
BMW i3	3,4
Tesla Model X	5,6
Chevrolet Bolt	7,8
Mercedes EQC	9,10

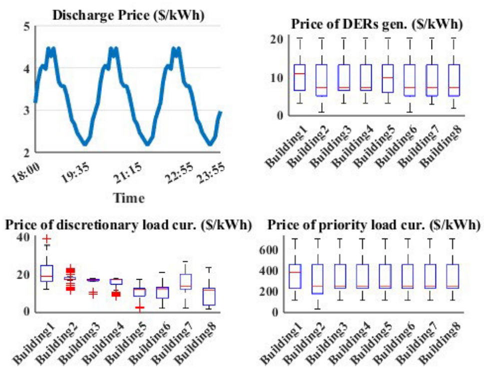

Fig. 6. Price data including discharge price, price of DER generation, price of discretionary and priority load curtailment.

With careful consideration of the motivations of EV owners, in most emergency cases, individuals typically do not seek solely to maximize their profit. Hence, if the preferences of EV owners are met (for example, if the SoE value becomes higher than SoE_{min} as discussed in section II-B), they would likely be willing to participate with a reasonable discharge price. As evidence, during Hurricane Sandy in 2012, many EV owners in the affected area lent their vehicles to provide electricity to hospitals, shelters, and charging stations for people's devices, see [43]. Hence, it would be rational to consider the EV discharge price to be lower than discretionary load curtailment and local DER prices in emergency cases, as shown in Fig. 6. Additionally, as depicted in Fig. 6, the prices considered for priority loads are higher than those for discretionary loads and DERs.

B. Results and Discussion

The implemented model (Equations (1)-(16) and (18)-(23)) contains 17 blocks of equations, 22,341 single equations, 9 blocks of variables, 15,006 single variables, 59,007 non-zero elements, and 5,760 discrete variables. After solving the MILP problem, the optimal value for the objective function C_{PEM}^{DA} obtained equal to \$2421.497. Without using EVs, the objective function would be \$8821.44, i.e., deploying EVs, in this case, the study reduces PEM strategy cost by about 72.55%. Moreover, there would be priority load curtailment in contrast to the case with EV. Table III shows the value of priority load curtailments. This finding confirms the conclusions of previous research such as [18] that showed the effectiveness of using EVs in PEM in extreme events.

The power balance between the total amount of curtailment and the load curtailments that are devoted to the buildings is

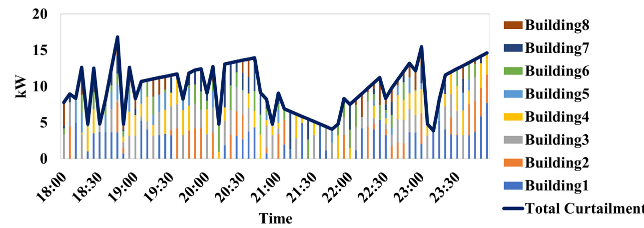

Fig. 7. Curtailment assignment to each building in Case A.

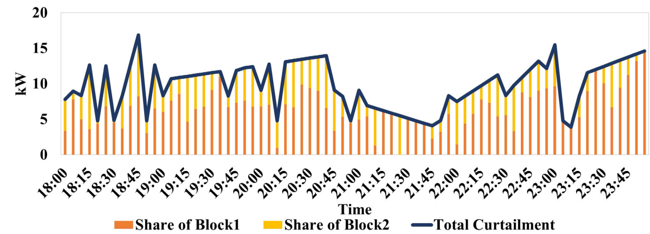

Fig. 8. Share of each block in curtailment.

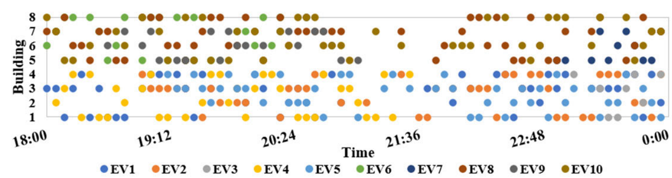

Fig. 9. EV services in the buildings located in City Block 1.

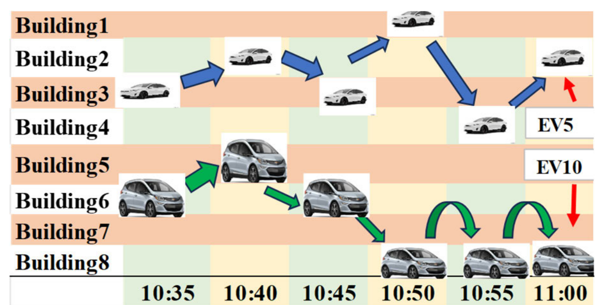

Fig. 10. EV5 and 10 services in different buildings.

shown in Fig. 7. This result confirms that the PEM strategy was able to successfully meet the curtailment requirement imposed by the TSO/DSO. The percentage of assigned curtailment to each block is depicted in Fig. 8. On average, the share of block 1 is 67% and the share of block 2 is 33%. Figure 9 shows the scheduled EV services in the buildings of City Block 1, throughout the energy service period. To better demonstrate the EV services in the building, another schematic is depicted in Fig.10. It is noted that as we stated previously, the city blocks are clustered in a way that the traveling time of EVs between the buildings is ignorable.

Figure 11 shows the discharging power of EVs in city block 1. On the right side of Fig. 11, we depict the discharge power for EV5 and EV10. The maximum value for discharging power of EV5 is 8.1116 kW and happened at 23:55 in building 1. For EV10, this value is 5.5221 kW and happened at 21:10 in building 7. The sum of EV discharge power in Blocks 1 and 2 is illustrated in Fig. 11. In Block 1, the maximum

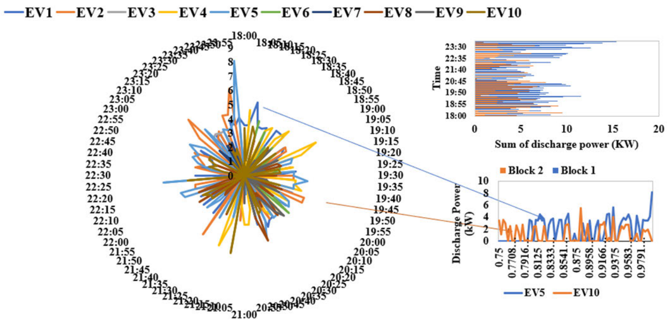

Fig. 11. EV discharge power in City Block 1.

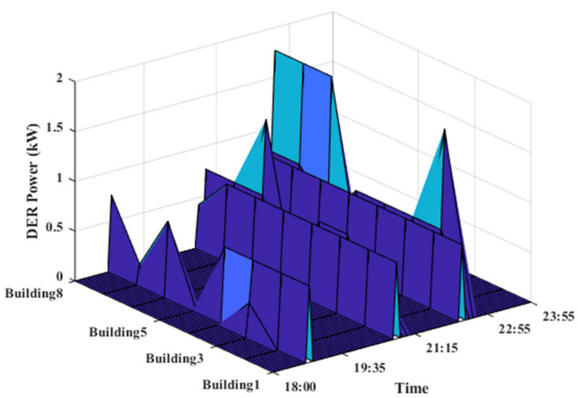

Fig. 12. Purchased power from local DERs.

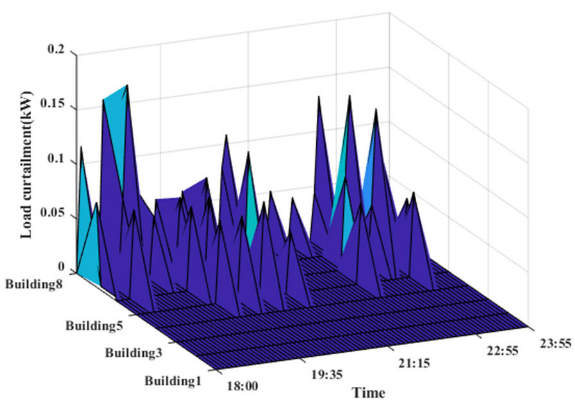

Fig. 13. Decreasing discretionary loads of buildings.

TABLE III

PRIORITY LOAD CURTAILMENT IN THE CASE WITHOUT EV

	18:45	19:35	19:50	23:35	23:40	23:45	23:50	23:55
Building 1	0	0.78	0	0	0	0.31	1.18	0
Building 2	0	0	0	0.49	0	1.1	0	0
Building 3	0.39	0	0	0	0	0	1.094	0
Building 4	0	0	0	0	0	1.13	0.76	0
Building 5	0.43	0	0	0	0	0	0.778	0
Building 6	0	0	0	0	0	0.65	0	0
Building 7	0.73	0	0	0	0	0	0	0
Building 8	0.85	0	0.65	0	0	0	0	0

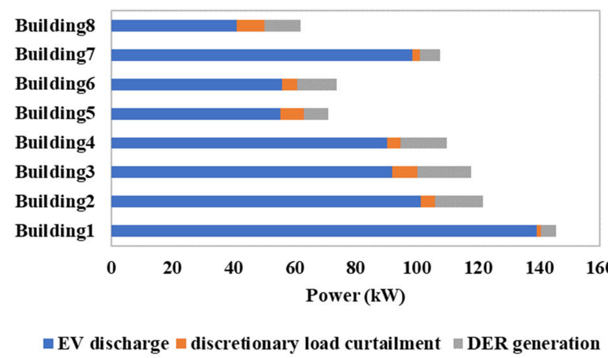

Fig. 14. The share of each party in load curtailment of each building (Case B).

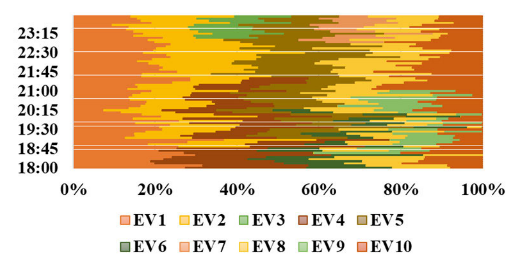

Fig. 15. The share of EVs' in discharge power in each hour.

discharge power was 15.3581kW at 23:55. This value is 9.5011 kW at 18:15. In Fig. 8, we depicted the share of each block in curtailment. It is observed that the peak for curtailment share occurred at 23:55 and 18:15 for Blocks 1 and 2, respectively. This means that for each block the peak of discharging has happened in the peak of curtailment share. Also, it is observed that at 18:50, we have no EV discharging in either block. Further investigation reveals that the price of DER generation at 18:50 (3.064 $/kWh) is less than that discharge price (3.668 $/kWh). Hence, at 18:50, we have DER generation instead of EV penetration. The purchased power from local DERs is shown in Fig. 12. The decreasing power of discretionary loads is shown in Fig. 13.

According to equations (2), (16), and (17), the curtailed load (shown in Fig. 8) should be compensated by DER power (shown in Fig. 12), decreased load (shown in Fig. 13), and EV discharging. It is noted that the value of priority load curtailment is zero. The results indicate that due to the participation of EVs in the PEM strategy, the share of DER power and decreased power of buildings is lower than the share of EV discharging.

For Case B, the obtained PEM cost is $3243.315. The share of EV discharge, DER generation, and load decrease in meeting the curtailment requirement of each building are shown in Fig. 14. As observed, the contribution of EV discharge power is greater than that of load curtailment and DER generation. It is confirmed that if there is proper motivation for increasing EVs' willingness in participation for energy services in extreme weather events, their role would be highlighted in an optimal PEM strategy. The share of each EV in total dispatch power in each hour is shown in Fig. 15.

It is evident from this figure that the number of hours each EV is willing to participate directly affects its share in hourly discharge power. For instance, EV3 and EV7 have a limited contribution to the total discharge power because their participation hours are less than others (55 and 65 minutes, respectively).

On the day of extreme weather event occurrence, the ECSC is notified that EV6 and EV9 participate by 10 minutes of delay i.e. instead of 18:00 and 18:35, they will participate at 18:10 and 18:45. The ECSC should perform rescheduling by solving optimization model of (44)-(53) for periods $[18:00\ 18:10]$ and $[18:35\ 18:40]$. Since $\propto_{e6,8,18:00} = 1$ and $\propto_{e9,6,18:35} = 1$, rescheduling should be performed in Buildings 8 and 6 respectively. In these periods, the lack of discharge power of EV6 (1.692632 kW) and EV9 (1.305263 kW) should be compensated for by more DERs generations and more decreasing power in these buildings. By implementing optimization model ((44)-(53)), $P^{RESCH\_DER}_{8,18:00} = 1.692632\ kW$, $P^{RESCH\_DER}_{6,18:35} = 1.2335\ kW$, and $P^{RESCH\_Ddown}_{6,18:35} = 0.071763\ kW$. Since these rescheduling periods have no intersection, cost allocation is not required and the rescheduling cost of the first and second periods should be paid by EV6 and EV9, respectively.

C. Scalability Management

Since the developed models of Case A and B are MILP, the complexity of the problem will be increased by increasing the number of binary variables. The number of binary variables $\propto_{e,b,t}$ is increased by increasing the number of EVs, the number of buildings, and the number of t. The problem is more severe for Case A. For example, in the discussed case of subsection B, we have 10 EVs, 8 buildings and 72 intervals (based on 5 min granularity) for Case A. Hence, we have $10 \times 8 \times 72 = 5760$ binary variables. By increasing the number of EVs and buildings, the number of binary variables increases, and the computational complexity is increased thereafter. Two solution approaches are proposed to reduce the complexity: (i) Reducing the number of intervals by decreasing time granularity: In the above case studies and scenarios, we consider 72 intervals based on $\Delta T = 5$ min. By increasing the size of the problem, we can increase ΔT. For a case study with the number of buildings and EVs equal to 20 and 16, if we consider $\Delta T = 20$ min. The number of integer variables would be the same as the previous case study $(20 \times 16 \times 18 = 5760)$, (ii) Using engineering-driven insights for converting Case A to Case B: As described in II-D, Case B provides detailed data on the amount of load curtailment for each building at every time period. As shown in II-D, (41)-(43) can be solved separately for each block and the computational effort decreases in comparison to that of Case A. One option is that if we have total load curtailment at time t in Case A ($\mathrm{P}^{\mathrm{CUR}}_{\mathrm{TOTAL},t}$), we can decompose it to obtain the amount of load curtailment in building b at time t ($P^{CUR}_{b,t}$) by collaboration of ECSC and households. As shown in Fig. 16, the share of each building from the curtailed load ($P^{CUR}_{b,t}$), is obtained by weight $\aleph_b$. To calculate $\aleph_b$, the collaboration between ECSC and households is required by adopting an engineering insight. To this end, the households give information about their loads to the ECSC and the ECSC determines the assigned weights ($\vartheta_{P,b}, \sigma_{D,b}$) to the priority and discretionary loads of all buildings, respectively.

In parallel, the households assign related weights to their priority and discretionary loads ($\varsigma_b$and$1 - \varsigma_b$), respectively.

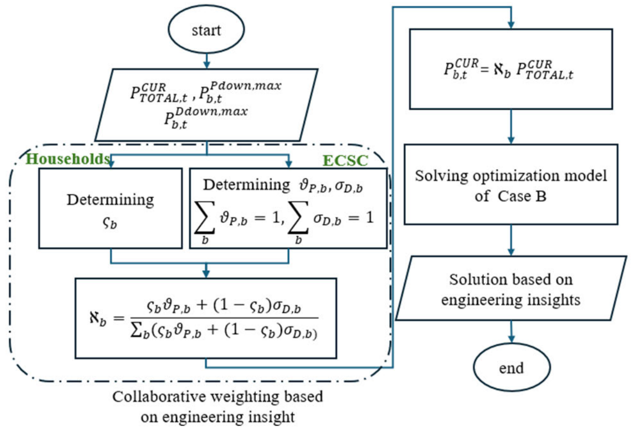

Fig. 16. Converting Case A to Case B for managing scalability.

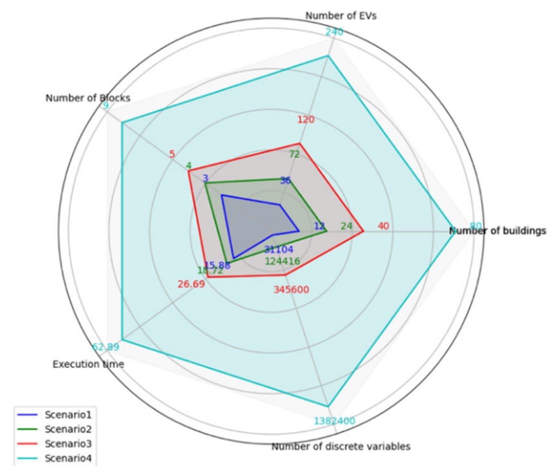

Fig. 17. Scalability test based on the algorithm of Fig. 16.

Finally, $\aleph_b$ is obtained through the collaborative weighting performed by ECSC and Households, as shown in Fig. 16. It is mentioned that the other forms of weighting can be designed for this purpose.

D. Comparison Analysis

In subsection B, while interpreting Fig. 15, we discover that the length of service time of EVs is significant and influences the PEM strategy. Now, we examine the arrival and departure times of each EV. The proposed PEM strategy is tested for Case A by changing the arrival and departure times of EVs without changing the length of service time. To this end, let us perform three tests by assuming different arrival and departure times of EVs 3 and 4.

Test1: $T^{sch}_{e3} = [23:0523:55]$, $T^{sch}_{e4} = [1821:30]$.
Test2: $T^{sch}_{e3} = [22:0522:55]$, $T^{sch}_{e4} = [1922:30]$.
Test3: $T^{sch}_{e3} = [21:0521:55]$, $T^{sch}_{e4} = [2023:30]$.

After conducting PEM for these tests, a few measures have been obtained and are listed in Table IV. Analysis of Table IV reveals that the preferences of EVs, such as arrival time and departure time, influence the measures of the PEM strategy.

Besides arrival and departure times, several opt-in preference metrics, such as the initial SoE, minimum SoE value, and service duration, influence the performance of PEM metrics.

TABLE IV
THE IMPACTS OF OPT-IN PREFERENCES OF EV3 AND 4

Period of service	PEM strategy Cost ($)	Average of decreased discretionary loads (kW)	Average discharge power of EVs(kW)	Average of curtailment shares	
				Block1	Block2
Test1	2421.50	0.0057	0.9774	66.70%	33.30%
Test2	2444.12	0.0093	0.9692	63.32%	36.68%
Test3	2427.43	0.0057	0.9738	68.19%	31.81%

One measure is the proportion of reserve energy that an EV offers ($SoE_e^{ini} - SoE_e^{min}$) divided by the total curtailed energy required in that period ($\int_{t_e^A}^{t_e^D} P_{TOTAL,t}^{CUR} dt$). Additionally, another measure is the proportion of service time to the total PEM service time ($\frac{t_e^D - t_e^A}{t^F - t^S}$). By multiplying these measures, a single index named the Resiliency-based Value of EV Opt-in (RVEO) is defined, which aggregates all opt-in preference metrics:

$$RVEO_e = \frac{SoE_e^{ini} - SoE_e^{min}}{\int_{t_e^A}^{t_e^D} P_{TOTAL,t}^{CUR} dt} \cdot \frac{t_e^D - t_e^A}{t^F - t^S} \tag{55}$$

In continuation, we are going to evaluate the impact of RVEO on the PEM's major indices. For this purpose, we will assess a few scenarios. As shown in Table V, the scenarios are designed in a way that by increasing the number of EVs and buildings, the value of RVEO decreases. To address scalability, we adopted transforming Case A to Case B, as described in subsection C. We assume $\varsigma_b = 0.8$. Also, $\vartheta_{P,b}$ and $\sigma_{D,b}$ are equal for all buildings. The comparison results of Table V shows, first, the effectiveness of using EVs in comparison with the case without using EVs, and second, the importance of EV opt-in preferences and their impacts on the PEM's performance metrics. Table V shows the results for a set of scenarios where, by increasing the number of EVs without improving the average RVEO, the PEM performance deteriorates. Also, Fig. 17 shows the scalability tests. The results show that by converting Case A to Case B, the model can be solved in a reasonable execution time.

IV. CONCLUSION

In this work, we proposed a preventive energy management (PEM) strategy by modeling EV owners' opt-in preferences in the blocks of a smart city in responding to extreme weather events. Two case studies were introduced and modeled. Also, a rescheduling procedure along with a cost allocation mechanism has been proposed in case of uncertainty occurrence. The numerical results confirmed the conclusions of the previous research that showed the effectiveness of using EVs in PEM in extreme events in two ways: first, the less obtained optimal cost function, and second, less curtailment of priority loads. Moreover, the impacts of the length of period of service and opt-in preferences of EVs have been demonstrated in the results analysis. Besides the minimum of State of Energy (SoE) to avoid a range anxiety, opt-in preferences should be considered in any policy design for the promotion of Vehicle-to-Grid (V2G) or Vehicle-to-Building (V2B). These points are the main contributions that we modeled and examined through our numerical study. In future work, the provision of traveling possibilities among city blocks and its effect on the optimal resiliency-related cost can be investigated. In addition, modeling battery degradation in the PEM strategy can be taken into consideration.

REFERENCES

[1] United Nations. (May 2018). *Department of Economic and Social Affairs*. United Nations Dept. Econ. Social Affairs. [Online]. Available: https://www.un.org/development/desa/en/news/population/2018-revision-of-world-urbanization-prospects.html

[2] *Nearly 220,000 People Remain Without Power Across the Bay Area*. Accessed: Sep. 22, 2023. [Online]. Available: https://www.ktvu.com/news/nearly-220000-people-remain-without-power-across-the-bay-area

[3] S. Meerow, J. P. Newell, and M. Stults, "Defining urban resilience: A review," *Landscape Urban Planning*, vol. 147, pp. 38–49, Mar. 2016, doi: 10.1016/j.landurbplan.2015.11.011.

[4] E. E. Stasinos, D. N. Trakas, and N. D. Hatziargyriou, "Microgrids for power system resilience enhancement," *iEnergy*, vol. 1, no. 2, pp. 158–169, Jun. 2022.

[5] Y. Lin and Z. Bie, "Tri-level optimal hardening plan for a resilient distribution system considering reconfiguration and DG islanding," *Appl. Energy*, vol. 210, pp. 1266–1279, Jan. 2018.

[6] X. Jing, W. Qin, H. Yao, X. Han, and P. Wang, "Resilience-oriented planning strategy for the cyber-physical ADN under malicious attacks," *Appl. Energy*, vol. 353, Jan. 2024, Art. no. 122052.

[7] H. Hou et al., "Resilience enhancement of distribution network under typhoon disaster based on two-stage stochastic programming," *Appl. Energy*, vol. 338, May 2023, Art. no. 120892.

[8] M. Tian, Z. Dong, L. Gong, and X. Wang, "Line hardening strategies for resilient power systems considering cyber-topology interdependence," *Rel. Eng. Syst. Saf.*, vol. 241, Jan. 2024, Art. no. 109644, doi: 10.1016/j.ress.2023.109644.

[9] M. R. Salehizadeh, M. A. Koohbijari, H. Nouri, A. Taşcıkaraoğlu, O. Erdinç, and J. P. S. Catalão, "Bi-objective optimization model for optimal placement of thyristor-controlled series compensator devices," *Energies*, vol. 12, no. 13, p. 2601, Jul. 2019, doi: 10.3390/en12132601.

[10] H. Qiu, W. Gu, W. Sheng, L. Wang, Q. Sun, and Z. Wu, "Resilience-oriented multistage scheduling for power grids considering nonanticipativity under tropical cyclones," *IEEE Trans. Power Syst.*, vol. 38, no. 4, pp. 1–14, 2022.

[11] S. S. Gharehveran, S. Ghassemzadeh, and N. Rostami, "Two-stage resilience-constrained planning of coupled multi-energy microgrids in the presence of battery energy storages," *Sustain. Cities Soc.*, vol. 83, Aug. 2022, Art. no. 103952, doi: 10.1016/j.scs.2022.103952.

[12] M. Rajabzadeh and M. Kalantar, "Improving the resilience of distribution network in coming across seismic damage using mobile battery energy storage system," *J. Energy Storage*, vol. 52, Aug. 2022, Art. no. 104891.

[13] T. Ding, M. Qu, Z. Wang, B. Chen, C. Chen, and M. Shahidehpour, "Power system resilience enhancement in typhoons using a three-stage day-ahead unit commitment," *IEEE Trans. Smart Grid*, vol. 12, no. 3, pp. 2153–2164, May 2021, doi: 10.1109/TSG.2020.3048234.

[14] Y. Wu, J. Wang, Y. Song, and Y. Xie, "Resilience-oriented valuation for energy storage amidst extreme events," *Chin. J. Electr. Eng.*, vol. 9, no. 3, pp. 15–25, Sep. 2023.

[15] J. Li, X. Xu, Z. Yan, H. Wang, M. Shahidehpour, and Y. Chen, "Coordinated optimization of emergency response resources in transportation-power distribution networks under extreme events," *IEEE Trans. Smart Grid*, vol. 14, no. 6, pp. 4607–4620, 2023.

[16] X. Cao, T. Cao, Z. Xu, B. Zeng, F. Gao, and X. Guan, "Resilience constrained scheduling of mobile emergency resources in electricity-hydrogen distribution network," *IEEE Trans. Sustain. Energy*, vol. 14, no. 2, pp. 1269–1284, Apr. 2023, doi: 10.1109/TSTE.2022.3217514.

[17] Z. Dong, X. Zhang, N. Zhang, C. Kang, and G. Strbac, "A distributed robust control strategy for electric vehicles to enhance resilience in urban energy systems," *Adv. Appl. Energy*, vol. 9, Feb. 2023, Art. no. 100115.

[18] L. Mauricette, Z. Dong, L. Zhang, X. Zhang, N. Zhang, and G. Strbac, "Resilience enhancement of urban energy systems via coordinated vehicle-to-grid control strategies," *CSEE J. Power Energy Syst.*, vol. 9, no. 2, pp. 433–443, Mar. 2023.

[19] T. Chowdhury, H. Chowdhury, K. S. Islam, A. Sharifi, R. Corkish, and S. M. Sait, "Resilience analysis of a PV/battery system of health care centres in rohingya refugee camp," *Energy*, vol. 263, Jan. 2023, Art. no. 125634.

[20] Y. Yang and S. Wang, "Resilient residential energy management with vehicle-to-home and photovoltaic uncertainty," *Int. J. Electr. Power Energy Syst.*, vol. 132, Nov. 2021, Art. no. 107206.

[21] A. K. Erenoglu, S. Sancar, I. S. Terzi, O. Erdinç, M. Shafie-Khah, and J. P. S. Catalão, "Resiliency-driven multi-step critical load restoration strategy integrating on-call electric vehicle fleet management services," *IEEE Trans. Smart Grid*, vol. 13, no. 4, pp. 3118–3132, Jul. 2022.

[22] H. Mehrjerdi, "Resilience oriented vehicle-to-home operation based on battery swapping mechanism," *Energy*, vol. 218, Mar. 2021, Art. no. 119528.

[23] M.-W. Tian and P. Talebizadehsardari, "Energy cost and efficiency analysis of building resilience against power outage by shared parking station for electric vehicles and demand response program," *Energy*, vol. 215, Jan. 2021, Art. no. 119058.

[24] Z. Zhao, C. K. M. Lee, J. Ren, and Y. P. Tsang, "Optimal EV fast charging station deployment based on a reinforcement learning framework," *IEEE Trans. Intell. Transp. Syst.*, vol. 24, no. 8, pp. 1–13, 2023.

[25] W. Feng et al., "A review of microgrid development in the United States—A decade of progress on policies, demonstrations, controls, and software tools," *Appl. Energy*, vol. 228, pp. 1656–1668, Oct. 2018.

[26] A. Hu, C. Shneider, A. Tiwari, and E. Camporeale, "Probabilistic prediction of dst storms one-day-ahead using full-disk SoHO images," *Space Weather*, vol. 20, no. 8, pp. 1–17, Aug. 2022.

[27] R. C. Yiyun and Y. Yao. (2023). *Outage Forecast-Based Preventative Scheduling Model for Distribution System Resilience Enhancement*. Accessed: Sep. 24, 2023. [Online]. Available: https://www.nrel.gov/docs/fy23osti/83982.pdf

[28] V. Sharma, T. Hong, V. Cecchi, A. Hofmann, and J. Y. Lee. (2023). *Forecasting Weather-Related Power Outages Using Weighted Logistic Regression*. IET Smart Grid. Accessed: Oct. 8, 2023. [Online]. Available: https://ietresearch.onlinelibrary.wiley.com/doi/pdfdirect/10.1049/stg2.12109

[29] J. Owens, I. Miller, and E. Gençer, "Can vehicle-to-grid facilitate the transition to low carbon energy systems?" *Energy Adv.*, vol. 1, no. 12, pp. 984–998, 2022.

[30] J. Geske and D. Schumann, "Willing to participate in vehicle-to-grid (V2G)? Why not!" *Energy Policy*, vol. 120, pp. 392–401, Sep. 2018.

[31] M. Mehdizadeh, T. Nordfjaern, and C. A. Klöckner, "Estimating financial compensation and minimum guaranteed charge for vehicle-to-grid technology," *Energy Policy*, vol. 180, Sep. 2023, Art. no. 113649.

[32] *Reversing the Charge—Battery Power From Electric Vehicles to the Grid Could Open a Fast Lane to a Net-Zero Future*. Accessed: Nov. 7, 2022. [Online]. Available: https://energy.mit.edu/news/reversing-the-charge/

[33] A. K. Erenoglu and O. Erdinç, "Real-time allocation of multi-mobile resources in integrated distribution and transportation systems for resilient electrical grid," *IEEE Trans. Power Del.*, vol. 38, no. 2, pp. 1108–1119, Apr. 2023.

[34] P. Jamborsalamati, M. J. Hossain, S. Taghizadeh, G. Konstantinou, M. Manbachi, and P. Dehghanian, "Enhancing power grid resilience through an IEC61850-based EV-assisted load restoration," *IEEE Trans. Ind. Informat.*, vol. 16, no. 3, pp. 1799–1810, Mar. 2020.

[35] W. Gan, J. Wen, M. Yan, Y. Zhou, and W. Yao, "Enhancing resilience with electric vehicles charging redispatching and vehicle-to-grid in traffic-electric networks," *IEEE Trans. Ind. Appl.*, vol. 60, no. 1, pp. 1–11, 2023.

[36] A. K. Candan, A. R. Boynuegri, and N. Onat, "Home energy management system for enhancing grid resiliency in post-disaster recovery period using electric vehicle," *Sustain. Energy, Grids Netw.*, vol. 34, Jun. 2023, Art. no. 101015.

[37] C. Lewis, "Value-of-resilience from solar microgrids: VOR123 methodology," *Clean Coalition*, vol. 5, pp. 1–30, Nov. 2020.

[38] L. P. Thomas Hancock. (2021). *Analysis of the Microgrid Market for Small and Medium-Sized Municipalities and Electric Cooperatives*. Duke University. Accessed: Oct. 3, 2023. [Online]. Available: https://dukespace.lib.duke.edu/dspace/bitstream/handle/10161/22696/MunicipalMicrogrid_FINAL_20210430.pdf?sequence=1

[39] G. Muñoz-Delgado, J. Contreras, J. M. Arroyo, A. Sanchez de la Nieta, and M. Gibescu, "Integrated transmission and distribution system expansion planning under uncertainty," *IEEE Trans. Smart Grid*, vol. 12, no. 5, pp. 4113–4125, Sep. 2021.

[40] S. Binato, M. V. F. Pereira, and S. Granville, "A new benders decomposition approach to solve power transmission network design problems," *IEEE Trans. Power Syst.*, vol. 16, no. 2, pp. 235–240, May 2001.

[41] *CPLEX*. Accessed: Sep. 19, 2023. [Online]. Available: https://www.gams.com/latest/docs/S_CPLEX.html

[42] H. C. Güldorum, I. Şengör, and O. Erdinç, "Management strategy for V2X equipped EV parking lot considering uncertainties with LSTM model," *Electr. Power Syst. Res.*, vol. 212, Nov. 2022, Art. no. 108248.

[43] BRADLEY BERMAN. (2012). *Electric Car Owners Unfazed by Storm*. Accessed: Sep. 30, 2023. [Online]. Available: https://archive.nytimes.com/wheels.blogs.nytimes.com/2012/11/02/electric-car-owners-unfazed-by-storm/

Mohammad Reza Salehizadeh (Senior Member, IEEE) is currently a Research Professor (Senior Research Fellow) with the Intelligent System Laboratory, Institute of Cleaner Production, Pukyong National University (PKNU), Busan, South Korea. Previously, he held the position of an Assistant Professor with the Electrical Engineering Department, Islamic Azad University, Marvdasht Branch, Iran. He is the Founder and a Leader of the Smart Systems Research Group (SSRG), Islamic Azad University. With over 19 years of experience, his expertise spans research, teaching, research and development, consulting, design, and simulation in areas, such as electricity markets, smart grids, power systems, optimization, decision-making, and control. He is the co-editor of the book titled *Hydrogen and e-Mobility: Technologies, Integration, and Optimal Management* (Elsevier). He is frequently invited to review submissions for leading journals in power and energy systems. His primary research interests include electric vehicles, smart grids, power system operation and planning, electricity markets, and decision-making. He has served as a Guest Editor for journals, including *IET Smart Cities*, *Energies*, *Sustainable Energy*, *Grids and Networks* (SEGAN), *Journal of Control*, and *Sustainable Energy Technologies and Assessments* (SETA).

Ayşe Kübra Erenoğlu (Member, IEEE) received the B.Sc., M.Sc., and Ph.D. degrees from Yıldız Technical University (YTU), Istanbul, Türkiye, in 2016, 2018, and 2021, respectively. In April 2017, she joined the Department of Electrical Engineering, YTU, as a Research Assistant, and subsequently assumed the position of an Assistant Professor with the Department of Electrical and Electronics Engineering, Fatih Sultan Mehmet Vakif University (FSMVU), in November 2022. She holds the position of the Vice Chair with the Department of Electrical and Electronics Engineering, FSMVU. She is currently an Assistant Professor with the Department of Electrical Engineering, YTU. Additionally, she is the University-Industry Collaboration Coordinator with the Institute of Clean Energy Technologies. Her research interests are power system resiliency, smart grid applications, renewable energy integration, and electric vehicles. She serves as the Treasurer for the Turkey Chapter of the IEEE Power and Energy Society (PES). She has served as the technical program committee member for IEEE co-sponsored conferences.

İbrahim Şengör (Senior Member, IEEE) received the B.Sc. degree in electrical engineering from Istanbul Technical University (ITU) in 2013 and the M.Sc. and Ph.D. degrees in electrical engineering from Yıldız Technical University (YTU), Istanbul, Türkiye, in 2016 and 2019, respectively. He was a Research Assistant and a Teaching Assistant with the Electrical Engineering Department, YTU, during his graduate studies. He was an Assistant Professor of electric power engineering with Izmir Katip Celebi University (IKCU), Izmir, Türkiye, from 2019 to 2022. He was a Post-Doctoral Research Fellow in electrification of transport and heating within the electric power system with the MaREI and the SFI Centre, University College Cork (UCC), Cork, Ireland from June 2021 to September 2023. He has been a Lecturer with the Department of Electrical and Electronic Engineering, Munster Technological University (MTU), Cork, since September 2023. His research interests include integration of electric vehicles, renewable energy systems to electric power grids, and power system operation within the smart grid concept.

Akın Taşçıkaraoğlu (Senior Member, IEEE) received the B.Sc., M.Sc., and Ph.D. degrees from Yıldız Technical University, Istanbul, Türkiye, in 2006, 2008, and 2013, respectively. From 2012 to 2017, he was a Researcher with the Department of Electrical Engineering, Yıldız Technical University. From 2014 to 2015, he was also a Post-Doctoral Scholar with the University of California at Berkeley. He is currently an Associate Professor with Mugla Sitki Kocman University, Mugla, Türkiye; and a Visiting Professor with the University of California at San Diego. He is a co-editor of the book titled *Pathways to a Smarter Power System* (Academic Press, 2019). He was a recipient of the Turkish Science Academy Distinguished Young Scientist Award (TUBA GEBIP) in 2021. He is an Editor of several journals, including IEEE SYSTEMS JOURNAL, IEEE ACCESS, *IET Renewable Power Generation*, *Turkish Journal of Electrical Engineering Computer Sciences*, and *e-Prime* (Elsevier).

Ozan Erdinç (Senior Member, IEEE) received the B.Sc., M.Sc., and Ph.D. degrees from Yıldız Technical University (YTU), Istanbul, Türkiye, in 2007, 2009, and 2012, respectively. Until May 2013, he was with private sector in different positions, including electrical installations, renewable energy investments, and as a procurement expert. In June 2013, he became a Post-Doctoral Fellow in Portugal, under the EU-FP7 funded SINGULAR Project. Later, he joined the Department of Electrical Engineering, YTU, where he obtained the title of an Associate Professor in April 2016. In September 2021, he was appointed as a Full Professor with YTU. He was the IEEE Power and Energy Society (PES) Turkey Chapter Chair; the Head of Alternative Energy Based Electric Systems Division, Department of Electrical Engineering, YTU; and the Director of Energy Application and Research Center, YTU. He is currently the Head of IT Department, YTU. His research interests are hybrid renewable energy systems, electric vehicles, power system operation, and smart grid technologies.

Jay Liu received the B.S. and M.S. degrees in chemical engineering from POSTECH, South Korea, in 1996 and 1998, respectively, and the Ph.D. degree from McMaster University, Canada, in 2004. He is a Full Professor with the Department of Chemical Engineering, Pukyong National University, South Korea. After working as a Process Design Engineer with Samsung E&A Company Ltd., South Korea, for over two years, then he entered McMaster University, where he studied process systems engineering under the supervision of Prof. John F. MacGregor. Upon obtaining the Ph.D. degree, he continued his research with the McMaster Advanced Control Consortium, McMaster University, as a Post-Doctoral Fellow. Then, he joined Samsung Electronics Company Ltd., South Korea, as a Senior Research Engineer. Since moving to academia in 2009, his research interests have focused on understanding underlying phenomena in chemistry and chemical engineering problems with the aid of data-driven and first principle-based modelling approaches. For more than 15 years his focus has been on design and analysis of sustainable energy systems and has published more than 90 research articles in academic journals, including *Chemical Reviews* and *Energy and Environmental Science*. He received several prestigious grants, fellowships, citations and awards, including the Samsung Fellowship in 1996; the Shell Canada Research Fellowship in 2003; the Young Researchers Grant at the Gordon Research Conference in 2003; the Minister's Citation by the Ministry of Trade, Industry and Energy of Korea, in 2014; the Beomseok Award by the Korean Institute of Chemical Engineers in 2017; the Mayor of Busan Metropolitan City in 2018; the Rector's Award by Nicolaus Copernicus University, Poland, in 2018; and the Minister's Citation by the Ministry of Science and ICT of Korea in 2023. One of his research outcomes on sustainable energy has been selected as one of the Top 100 National Research and Development Outstanding Achievements by Korea Institute of S&T Evaluation and Planning in 2022.

João P. S. Catalão (Fellow, IEEE) is a Full Professor (Professor Catedrático) with the Faculty of Engineering, University of Porto, Portugal. He is a Highly Cited Researcher in the field of engineering. He is among the Top 2% of Scientists and a Best Scientist in Research.com. He was the Primary Coordinator of the 5.2-million-euro FP7-EU project SiNGULAR, from 2012 to 2015. Currently, he is the Primary Coordinator of the 4.5-million-euro Horizon-EU project EU-DREAM, from 2024 to 2027. He has co-authored more than 500 journal publications, with an H-index of 99 and more than 37,000 citations (according to Google Scholar), having supervised more than 130 researchers (post-docs, Ph.D. and M.Sc. students, and other students with project grants). He was an editor of two books, such as *Electric Power Systems: Advanced Forecasting Techniques and Optimal Generation Scheduling* (CRC Press, 2012); and *Smart and Sustainable Power Systems: Operations, Planning and Economics of Insular Electricity Grids* (CRC Press, 2015). His research interests include power system operations and planning, power system economics and electricity markets, distributed renewable generation, demand response, smart grids, and multi-energy carriers. He was an IEEE CIS Fellows Committee Member, from 2022 to 2024. He was elected as a Full Member of Sigma Xi, the Scientific Research Honor Society, in 2023. Furthermore, he has won five best paper awards at IEEE conferences. He was the General Chair of SEST 2019 (technically co-sponsored by IEEE) and the Inaugural Technical Chair and a Co-Founder of SEST 2018. He is a Senior Editor of IEEE TRANSACTIONS ON NEURAL NETWORKS AND LEARNING SYSTEMS; and IEEE TRANSACTIONS ON SYSTEMS, MAN, AND CYBERNETICS: SYSTEMS. He was recognized as an Outstanding Associate Editor in 2023 and 2021 for IEEE TRANSACTIONS ON EMERGING TOPICS IN COMPUTATIONAL INTELLIGENCE and IEEE TRANSACTIONS ON POWER SYSTEMS and an Outstanding Senior Associate Editor in 2020 for IEEE TRANSACTIONS ON SMART GRIDS.